

# Preparation and Electrochemical Performance of CMF High Voltage Cathode Material for Lithium Ion Battery

Jingbin Zhang\*, Ping Liu, Xiaofeng Bi

Hebei Vocational College of Rail Transportation, Shijiazhuang 052165, China  
 zhangjb129@126.com

In this paper, based on CMF high voltage and liquid precipitation method, the ternary precursor is prepared; then by mixing it with lithium carbonate, the analysis is made for their properties through the XRD and thermogravimetry; finally, the ternary cathode material of lithium ion battery is prepared under the high temperature reaction for the mixture of the precursors and lithium carbonate, and the electrochemical properties of the material are investigated. The oxidative dehydration process of the ternary precursor is mainly concentrated at 250°C-350°C under the CMF high voltage. As the temperature increases to 200°C and 300°C respectively, the ternary precursors are developed into  $\text{Me}(\text{OH})_2$  and  $\text{CoNiOOH}$  structures respectively; as the temperature further increases  $\text{CoNiOOH}$  was anhydrated into  $\text{Mn}(\text{Ni, Co})_2\text{O}_4$ , and the material surface becomes very dense; at 300-500°C, the mixture shows the characteristics of the composite oxide ( $\text{LiNi}_{0.5}\text{Co}_{0.2}\text{Mn}_{0.3}\text{O}_2$ ); at 600°C above, the diffraction peak belonging to lithium carbonate completely disappears, and  $\text{LiNi}_{0.5}\text{Co}_{0.2}\text{Mn}_{0.3}\text{O}_2$  is basically generated. The electrochemical analysis of  $\text{LiNi}_{0.5}\text{Co}_{0.2}\text{Mn}_{0.3}\text{O}_2$  shows that the maximum specific capacity of the battery for the first charge and discharge is 172 mAh/g, and the Coulomb efficiency is 90.1%. When the lithium content in the material is set to be 1.09, the battery parameters such as median voltage and discharge platform all reach the optimal value.

## 1. Introduction

Lithium-ion batteries have been widely used in various electronic products (computer, mobile phone, MP3, etc.) and vehicles (electric car, electric motorcycle, etc.) due to their excellent performance. Lithium-ion batteries have a huge market space and a wide range of applications prospect. Now all countries in the world have invested much capital to promote the innovation of lithium-ion battery technology (Zhao et al., 2017; Yoshio and Noguchi, 2009).

Lithium cobalt oxide is the core cathode material for lithium-ion battery, but its high cost and toxic property limit the development of lithium-ion battery (Mamyrbayeva et al., 2014; Hui and Zhou, 2006). The development of alternative materials for lithium cobalt oxide is the focus of current research, and in the existing literature,  $\text{LiNiO}_2$ ,  $\text{LiMn}_2\text{O}_4$ , and  $\text{LiNi}_x\text{Co}_{1-x}\text{O}_2$  have been studied as alternatives to lithium cobalt oxide (Hosono et al., 2009; Ding et al., 2011), but both  $\text{LiNiO}_2$  and  $\text{LiMn}_2\text{O}_4$  have poorer anti-high temperature property.  $\text{LiNi}_x\text{Co}_{1-x}\text{O}_2$  is the optimized material for the two materials mentioned above, but with unstable structure, the mixing arrangement of sodium ions and lithium ions makes it difficult to synthesize its stoichiometric ratio (Li et al., 2008; He et al., 2005; Chen et al., 2003; Ohzuku and Makimura, 2001; Yabuuchi and Ohzuku, 2003).

$\text{LiNi}_x\text{Co}_y\text{Mn}_{1-x-y}\text{O}_2$  is a new type of ternary composite oxidized material proposed in recent years (Wang et al., 2009; Liao and Duh, 2005), with large capacity, excellent cycle performance, and stable structure of  $\text{LiNiO}_2$ ,  $\text{LiMn}_2\text{O}_4$ , and  $\text{LiCoO}_2$ . It is known so far to be the best cathode material of lithium-ion battery (Li et al., 2005; Wang et al., 2002; Lee et al., 2010). At present, the related researches on  $\text{LiNi}_x\text{Co}_y\text{Mn}_{1-x-y}\text{O}_2$  material still remains at the primary stage; further research should be conducted on the positive electrode distribution of lithium ion battery, the property change of particles at high temperature, tap density, static and dynamic mechanical property (Hwang et al., 2003; Yuan and Ying, 2002).

In this paper, based on CMF high voltage and liquid precipitation method, the ternary precursor is prepared; then by mixing it with lithium carbonate, the analysis is made for their properties through the XRD and thermogravimetry; finally, the ternary cathode material of lithium ion battery is prepared under the high

temperature reaction for the mixture of the precursors and lithium carbonate, and the electrochemical properties of the material are investigated.

## 2. Test materials and method

### 2.1 Preparation of test materials

Raw materials were prepared, including: nickel sulphate, manganese sulphate,  $\text{CoCl}_2$ , sodium hydroxide, and ammonia; these materials were mixed and stirred in a certain proportion to obtain the nickel-cobalt-manganese composite precipitate; the precipitate was washed and dried to obtain the ternary precursor of  $\text{Ni}_{0.5}\text{Co}_{0.2}\text{Mn}_{0.3}(\text{OH})_2$  (Sample 1); the ratio of the main chemical composition is Ni: 30.55%; Co: 13.12%; Mn: 17.55%.

Sample 1 was mixed with lithium carbonate to obtain Sample 2. The two samples were heat treated separately and cooled for later use.

### 2.2 Material characterization and test methods

Thermogravimetry: use NETZSCH thermal analyser, at the heating rate  $12\text{ }^\circ\text{C}/\text{min}$ ;

XRD test: Use Bruker X-ray diffractometer, at scan rate  $5^\circ/\text{min}$  with scan range  $10\text{-}90^\circ$ ;

Electrical performance test: adopt the charge and discharge performance of battery cycle test material, at voltage:  $2.5\text{-}4.5\text{V}$ , at the charge and discharge rate of  $0.5\text{C}$ .

## 3. Test results and analysis

### 3.1 Performance analysis of ternary precursors and mixtures

Fig.1 depicts the thermogravimetric test curve for the prepared ternary precursor (Fig.1(a)) and its mixture with lithium carbonate (Fig.1(b)). It can be seen in figure that when the temperature is increased to  $300^\circ\text{C}$ , the total mass of sample 1 is lost by about 4.6%. The main reaction occurring in the ternary precursor can be expressed as:

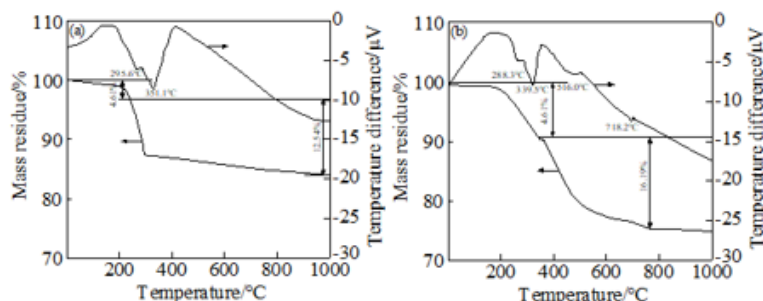
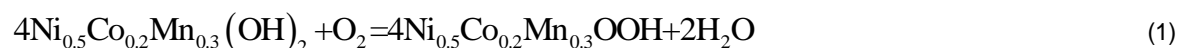


Figure 1: Thermogravimetric test curve for the prepared ternary precursor and its mixture

With the temperature further increasing, Sample 1 started oxidation and dehydration process according to formula (2), and the reaction was accompanied by vast endothermic and continuous mass loss.



On the whole the oxidative dehydration process of the ternary precursors is mainly concentrated at  $250^\circ\text{C}$ - $350^\circ\text{C}$ .

As seen from Fig. 1(b), the thermogravimetry curve of the mixture is similar to that of Fig. 1(a), and there are also two endothermic peaks with mass loss of about 8.8%. The reaction for the entire oxidation dehydration process can be expressed as:



By comparing Fig. 1(a) with Fig. 1(b), it can be seen that the ternary precursor shows a steady change after 350°C, and the mixture shows two distinct endothermic peaks after 350°C, indicating that the reaction temperature of the mixture for sample 2 needs to be over 350°C.

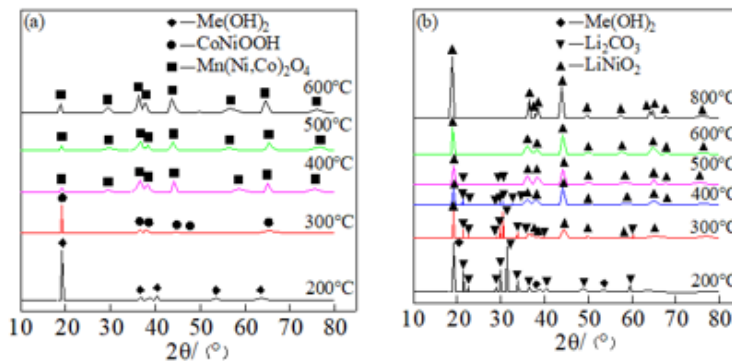


Figure 2: XRD curve for the ternary precursor and its mixture

Fig.2 depicts the XRD curve of the prepared ternary precursor (Fig.2(a)) and its mixture with lithium carbonate (Fig.2(b)). From Fig. 2(a), it can be seen that when the temperature is increased to 200°C and 300°C respectively, the ternary precursor forms  $\text{Me}(\text{OH})_2$  and  $\text{CoNiOOH}$  structure respectively; when the temperature further increases,  $\text{CoNiOOH}$  is anhydrated to  $\text{Mn}(\text{Ni, Co})\text{O}_4$ ; afterwards, the overall structure of the ternary precursor no longer changes when the temperature continues to increase.

For the mixture, below 300°C, the XRD spectrum of the mixture and the ternary precursor is basically the same; at 300-500°C, the mixture shows the characteristics of the composite oxide ( $\text{LiNi}_{0.5}\text{Co}_{0.2}\text{Mn}_{0.3}\text{O}_2$ ) with smaller diffraction peak in general, because the structure of lithium carbonate is damaged; at 600°C above, the diffraction peaks belonging to lithium carbonate completely disappear, and  $\text{LiNi}_{0.5}\text{Co}_{0.2}\text{Mn}_{0.3}\text{O}_2$  is completely formed, with obvious split peaks, when the entire material is distributed in layers.

### 3.2 $\text{LiNi}_{0.5}\text{Co}_{0.2}\text{Mn}_{0.3}\text{O}_2$ Electrochemical performance analysis

Fig.3 shows the X-ray diffraction spectrum of the prepared main cathode material: nickel-cobalt-manganese ( $\text{LiNi}_{0.5}\text{Co}_{0.2}\text{Mn}_{0.3}\text{O}_2$ ). Comparing Fig. 2 and Fig. 3, it can be seen that the structural distributions of nickel-cobalt-manganese (Ni-Co-Mn) and lithium nickelate are substantially the same and both have the  $\alpha\text{-NaFeO}_2$  structure; besides, the main peaks of Ni-Co-Mn prepared at peak 006 and 108 are split obviously, which can further reduce the appropriate temperature for the preparation of nickel cobalt manganese to be 760-860 °C.

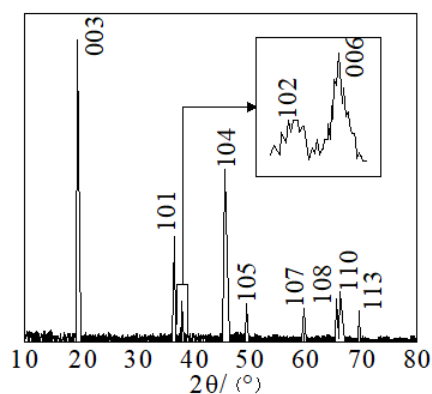


Figure 3: X-ray diffraction spectrum of cobalt

$\text{LiNi}_{0.5}\text{Co}_{0.2}\text{Mn}_{0.3}\text{O}_2$

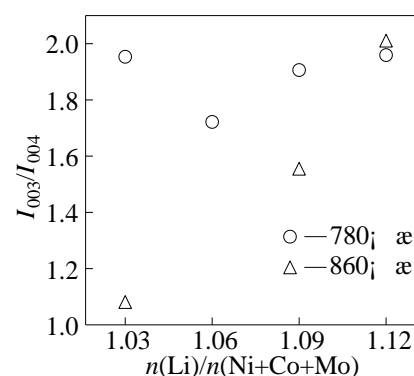


Figure 4: Ratio of 003 peak and 104 peak for nickel, and manganese under different lithium contents

The ratio R of the 003 peak and the 104 peak in Fig. 3 was calculated, and the calculation result is shown in Fig. 4. The existing studies have shown that the smaller the R value, the more unstable the cations in Ni-Co-

Mn, and the worse the electrochemical performance, generally by using  $R=1.2$  as the demarcation point. It can be seen from the figure that when the lithium ion content in Ni-Co-Mn gradually increases, the  $R$  value gradually increases; at the ambient temperature  $780\text{ }^{\circ}\text{C}$ , the  $R$  value does not meet the conditions, and the electrochemical properties of Ni-Co-Mn are poor; as the ambient temperature increases to  $860\text{ }^{\circ}\text{C}$ , the  $R$  values under the four kinds of lithium ion content meet the requirements, indicating that increasing the lithium ion content of cathode material and calcination temperature both contribute to the stability of the cations.

Fig.5 depicts the charge-discharge curve of Ni-Co-Mn under the first cycle and multiple cycles. From Fig. 5(a), it can be seen that the maximum specific capacity of the battery for the first charge and discharge is  $172\text{mAh/g}$ , and the Coulomb efficiency is  $90.1\%$ . From Fig. 5(b), when the specific capacity is  $150\text{-}170\text{mAh/g}$ , there was no decay in battery capacity for a total of 30 cycles, and the entire curve has only one platform. Besides, the discharge specific capacity of Ni-Co-Mn is less than in 10-20 charge-discharge cycles during 1-9 charge-discharge cycles, which is due to the activation phenomenon of the cathode material.

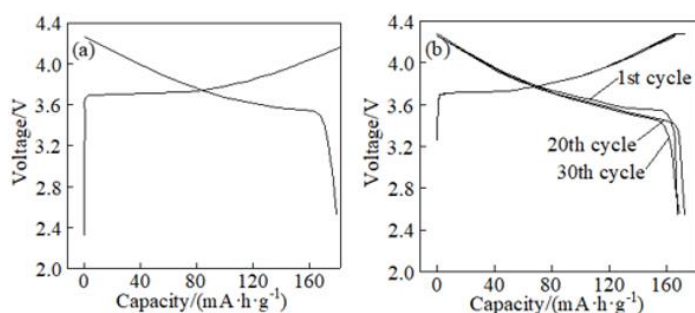


Figure 5: Charge-discharge curve of nickel, cobalt and manganese under the first cycle and multiple cycles

The effects of different number of charge-discharge cycles on the discharge specific capacity were investigated under the four kinds of lithium ion content (1.03, 1.06, 1.09, 1.12) respectively (Table 1). It can be seen from the figure, as the lithium content increases, the maximum discharge specific capacity gradually decreases during the low number of charge and discharge cycles (2 times), and the discharge specific capacity increases and decreases after 10 to 30 charge-discharge cycles. That is because that the increase in lithium ion destroys the valence balance of  $\text{LiNi}_{0.5}\text{Co}_{0.2}\text{Mn}_{0.3}\text{O}_2$ , resulting in an increase in the proportion of  $\text{Ni}^{2+}$ , which further reduces the specific capacity; besides, the increase in lithium ions also reduces the random mixing of  $\text{Ni}^{2+}$  and  $\text{Li}^+$ ; but when the lithium ion content is too high, the excess lithium will decrease the capacity retention of the battery. Therefore, based on the above analysis, the lithium content should be set to 1.09.

The median voltage of battery and material density are closely related. Table 2 shows the effect of different charge-discharge cycles on the battery median voltage under the four lithium ion contents (1.03, 1.06, 1.09, 1.12). Fig.6 shows the average of median voltage by different charge and discharge cycles under the same lithium content. From Table 2 and Fig.6, it can be seen that when the lithium ion content is 1.06 to 1.09, the median voltage gradually increases, and the median voltage reaches a peak at 1.09; when the lithium ion content reaches 1.12, the median voltage is decreased, different from that at 1.09. According to the test results, setting the lithium content to 1.09 can ensure that the battery has an optimal median voltage.

Fig.7 shows the relationship between the discharge platform of the battery cathode material and the lithium content. It can be seen from the figure that the change in the discharge platform is the same as in the median voltage, showing the changing feature of "increasing first and then decreasing".

Table 1: Effect of different number of charge-discharge cycles on discharge specific capacity under four kinds of Lithium Ions contents

Sample	$n(\text{Li})/n(\text{Ni}+\text{Co}+\text{Mn})$	Discharge capacity/ $(\text{mA}\cdot\text{h}\cdot\text{g}^{-1})$					Decay rate/%
		Two cycle	Ten cycle	Twenty cycle	Thirty cycle	Forty cycle	
R(1.03)	1.03	169.9	170.7	162.9	158.9	154.3	0.22
R(1.06)	1.06	167.8	171.1	168.0	166.1	160.0	0.13
R(1.09)	1.09	169.2	166.6	162.9	163.2	163.3	0.10
R(1.12)	1.12	166.3	164.5	156.7	156.5		0.21

Table 2: Effect of different number of charge and discharge cycles on median voltage under four kinds of Lithium Ions contents

Sample	n(Li)/n(Ni+Co+Mn)	Discharge capacity/(mA·h·g <sup>-1</sup> )				
		Two cycle	Ten cycle	Twenty cycle	Thirty cycle	Forty cycle
R(1.03)	1.03	3.75	3.75	3.75	3.72	3.71
R(1.06)	1.06	3.76	3.75	3.74	3.75	3.72
R(1.09)	1.09	3.77	3.76	3.75	3.74	3.73
R(1.12)	1.12	3.79	3.77	3.74	3.76	

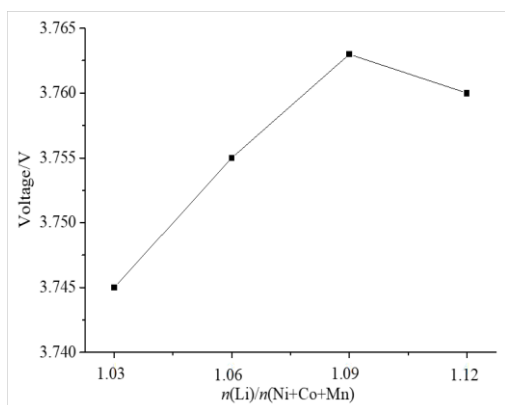


Figure 6: Curve of the mean voltage of under four kinds of Lithium Ions contents

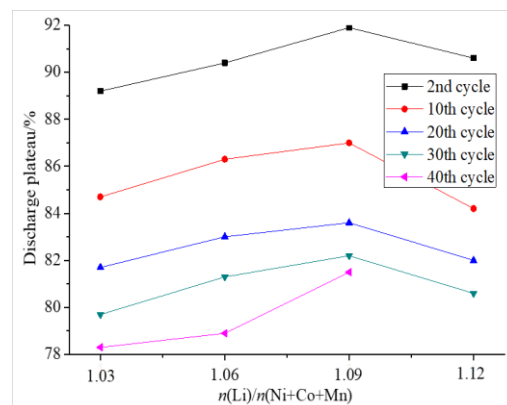


Figure 7: Change of discharge platform for different number of charge and discharge cycles under four kinds of lithium ion content

#### 4. Conclusion

In this paper, based on CMF high voltage and liquid precipitation method, the ternary precursor is prepared; then by mixing it with lithium carbonate, the analysis is made for their properties through the XRD and thermogravimetry; finally, the ternary cathode material of lithium ion battery is prepared under the high temperature reaction for the mixture of the precursors and lithium carbonate, and the electrochemical properties of the material are investigated. The conclusion is made as follows:

(1) The oxidative dehydration process of the ternary precursor is mainly concentrated in 250°C-350°C under the CMF high voltage. As the temperature is increased to 200°C and 300°C respectively, the ternary precursors are developed into Me(OH) and CoNiOOH structures respectively; as the temperature further increases, CoNiOOH was anhydrated into Mn(Ni, Co)2O4, and the material surface becomes very dense; at 300-500°C, the mixture shows the characteristics of the composite oxide (LiNi0.5Co0.2Mn0.3O2); at 600°C above, the diffraction peak belonging to lithium carbonate completely disappears, and LiNi0.5Co0.2Mn0.3O2 is basically generated.

(2) The electrochemical analysis of LiNi0.5Co0.2Mn0.3O2 shows that the maximum specific capacity of the battery for the first charge and discharge is 172 mAh/g, and the Coulomb efficiency is 90.1%. When the lithium content in the material is set to be 1.09, the battery parameters such as median voltage and discharge platform all reach the optimal value.

#### References

- Chen Y., Wang G.X., Konstantinov K., Liu, H.K., Dou S. X., 2003, Synthesis and characterization of LiCoxMnyNi1-x-yO2 as a cathode material for secondary lithium batteries, Journal of Power Sources, s 119-121(6), 184-188.
- Ding Y.L., Xie J., Cao G.S., Zhu T.J., Yu H.M., Zhao X.B., 2011, Single-crystalline LiMn2O4 nanotubes synthesized via template-engaged reaction as cathodes for high-power lithium ion batteries, Advanced Functional Materials, 21(2), 348-355, DOI:10.1002/adfm.201001448

- He X.M., Li J.J., Cai Y., Wang Y., Ying J., Jiang C., Wan C., 2005, Preparation of spherical spinel LiMn<sub>2</sub>O<sub>4</sub>, cathode material for lithium ion batteries, *Materials Chemistry & Physics*, 9(6), 438-444, DOI:10.4028/0-87849-410-3.477
- Hosono E., Kudo T., Honma I., Matsuda H., Zhou H., 2009, Synthesis of single crystalline spinel LiMn<sub>2</sub>O<sub>4</sub> nanowires for a lithium ion battery with high power density, *Nano Letters*, 9(3), 1045-1051, DOI:10.1021/nl803394v
- Hui X., Zhou Z., 2006, Physical and electrochemical properties of mix-doped lithium iron phosphate as cathode material for lithium ion battery, *Electrochimica Acta*, 51(10), 2063-2067, DOI:10.1016/j.electacta.2005.07.014
- Hwang B.J., Tsai Y.W., Chen C.H., Santhanam R., 2003, Influence of Mn content on the morphology and electrochemical performance of LiNi<sub>1-x</sub>CoxMnyO<sub>2</sub> cathode materials, *Journal of Materials Chemistry*, 13(8), 1962-1968, DOI:10.1039/b301468c
- Lee H.W., Muralidharan P., Ruffo R., Mari C.M., Cui Y., Kim d.K., 2010, Ultrathin spinel LiMn<sub>2</sub>O<sub>4</sub> nanowires as high power cathode materials for li-ion batteries. *Nano Letters*, 10(10), 3852-3856, DOI:10.1021/nl101047f
- Li D., Peng Z., Ren H., Guo W., Zhou Y., 2008, Synthesis and characterization of LiNi<sub>1-x</sub>CoxO<sub>2</sub>, for lithium batteries by a novel method, *Materials Chemistry & Physics*, 107(1), 171-176, DOI:10.1016/j.matchemphys.2007.06.069
- Li D., Sasaki Y., Kageyama M., Kobayakawa K., Sato Y., 2005, Structure, morphology and electrochemical properties of LiNi<sub>0.5</sub>Mn<sub>0.5-x</sub>CoxO<sub>2</sub>, prepared by solid state reaction. *Journal of Power Sources*, 148(2), 85-89, DOI:10.1016/j.jpowsour.2005.02.006
- Liao P.Y., Duh J.G., 2005, Synthesis and characterization of LiNixCoyMn1-x-yO<sub>2</sub> as a cathode material for lithium ion batteries, *Key Engineering Materials*, 280-283, 677-682.
- Mamyrbayeva Y.Y., Hobosyan M.A., Kumekov S.E., Martirosyan K.S., 2014, Electrochemical features of combustion-synthesized lithium cobaltate as cathode material for lithium ion battery, *International Journal of Self-Propagating High-Temperature Synthesis*, 23(1), 1-8, DOI:10.3103/s1061386214010087
- Ohzuku T., Makimura Y., 2001, Layered lithium insertion material of LiCo<sub>1/3</sub>Ni<sub>1/3</sub>Mn<sub>1/3</sub>O<sub>2</sub> for lithium-ion batteries. *Chemistry Letters*, 1(7), 642-643, DOI:10.1246/cl.2001.642
- Wang L., Li J., He X., Pu W., Wan C., Jiang C., 2009, Recent advances in layered LiNixCoyMn1-x-yO<sub>2</sub>, cathode materials for lithium ion batteries, *Journal of Solid State Electrochemistry*, 13(8), 1157-1164, DOI:10.1007/s10008-008-0671-7
- Wang Z., Liu L., Chen L., Huang X., 2002, Structural and electrochemical characterizations of surface-modified LiCoO<sub>2</sub> cathode materials for li-ion batteries, *Solid State Ionics*, 148(3), 335-342, DOI:10.1016/s0167-2738(02)00071-1
- Wu L., Yang G.S., Dai W.J., 2018, Parameter Determination of Lithium Titanate Battery for Rail Transit Based on Ocv-soc Characteristic Curve, *Chemical Engineering Transactions*, 66, 1321-1326, DOI: 10.3303/CET1866221
- Yabuuchi N., Ohzuku T., 2003, Novel lithium insertion material of LiCo<sub>1/3</sub>Ni<sub>1/3</sub>Mn<sub>1/3</sub>O<sub>2</sub> for advanced lithium-ion batteries, *Journal of Power Sources*, s 119-121(6), 171-174, DOI:10.1016/s0378-7753(03)00173-3
- Yoshio M., Noguchi H., 2009, A Review of Positive Electrode Materials for Lithium-Ion Batteries, *Lithium-Ion Batteries*, Springer New York, DOI: 10.1007/978-0-387-34445-4\_2
- Yuan W.Q., Ying X., 2002, Investigation of the local structure of the lini<sub>0.5</sub>Mn<sub>0.5</sub>O<sub>2</sub> cathode material during electrochemical cycling by X-ray absorption and nmr spectroscopy, *Electrochemical and Solid-State Letters*, 5(11), A263-A266, DOI: 10.1149/1.1513001
- Zhao Q., Lu Y., Chen J., 2017, Advanced organic electrode materials for rechargeable sodium-ion batteries, *Advanced Energy Materials*, 7, 1601792, DOI: 10.1002/aenm.201601792